within Sector Santa Rosa, Area de Conservacion, Guanacaste (ACG), of northwest Costa Rica[27]. In 1976, all stems ≥3 cm dbh were mapped within a continuous 680 m × 240 m (16.32 Ha) area of forest[20] by S. P. Hubbell. Using an identical mapping protocol, a second remap of the San Emilio forest was completed between 1995 and 1996. In total, 46,833 individuals have been surveyed, 26,960 in 1976 and 19,873 in 1996. Together, the two surveys document 20 yr of growth and population change for about 150 species. The plot is composed of secondary growth forest and is heterogeneous with respect to age, topography and degree of deciduousness.

Calculation of individual tree growth

In 1976, most trees greater than 10 cm dbh were tagged with aluminum tree markers and given a unique identification number. Because few smaller individuals were given aluminum tags in 1976, tree growth was usually followed only for those trees greater than 10 cm dbh. Growth was calculated by monitoring changes in dbh for each individual. To ensure an accurate estimate of growth, a species was included only if a minimum representation of seven individuals had initial stem diameters ≥10 cm, and the diameter range of all individuals ≥20 cm. As the minimum diameter cut off for individuals was 10 cm, this imposed a minimum size range of 30 cm. Only individuals experiencing positive growth in the 20-year period were used for the calculation of allometric equations. In some cases, individuals experienced no change or even a decrease in diameter over time. This was usually due to partial death, loss of the main trunk or measuring errors. The 45 species meeting the above criteria are listed in Table 1. Production equations for each species were generated by plotting $D^{2/3}(0)$ versus $D^{2/3}(20)$ on linear axes. Because dbh was measured identically in 1976 and 1996, measurement error is likely to be equally distributed across the x and y axes. For these reasons, allometric slopes were determined using Model II RMA regression[1,28,29]. Equations and statistics for each species are also reported in Table 1.

Species-specific wood density

The specific wood density, ρ, is a simple measure of the total dry mass per unit volume of wood (g cm^{-3}). The specific density of wood is closely related to mechanical properties of strength, such as elastic moduli, which describe resistance to static and impact bending, compression and tension[28]. For 29 of the 45 species reported in this study, values of specific wood density, ρ, in g cm^{-3}, were taken from the literature[24,26,30]. If more than one study reported a different value for a species, then the average value was used (Table 1).

1. Charnov, E. L. Life History Invariants: Some Explorations of Symmetry in Evolutionary Ecology (Oxford Univ. Press, Oxford, 1993).
2. Stearns, S. C. The Evolution of Life Histories (Oxford Univ. Press, Oxford, 1992).
3. Richards, P. W. The Tropical Rain Forest 2nd edn (Cambridge Univ. Press, Cambridge, 1996).
4. Chambers, J. Q., Higuchi, N. & Schimel, J. P. Ancient trees in Amazonia. Nature 391, 135–136 (1998).
5. Grime, J. P. & Hunt, R. Relative growth-rate: its range and adaptive significance in a local flora. J. Ecology 63, 393–422 (1975).
6. Tilman, D. Plant Strategies nd the Dynamics and Structure of Plant Communities (Princeton Univ. Press, Princeton, 1988).
7. Cebran, J. & Duarte, C. M. The dependence of herbivory on growth rate in natural plant communities. Func. Ecol. 8, 518–525 (1994).
8. Gleeson, S. K. & Tilman, D. Plant allocation, growth rate and successional status. Func. Ecol. 8, 543–550 (1994).
9. Ricklefs, R. E. Environmental heterogeneity and plant species diversity: an hypothesis. Am. Nat. 111, 376–381 (1977).
10. Grubb, P. J. The maintenance of species diversity in plant communities: the importance of the regeneration niche. Biol. Rev. 52, 107–145 (1977).
11. Denslow, J. S. Gap partitioning among tropical rain forest trees. Biotropica (Suppl.), 12, 47–55 (1980).
12. Williamson, G. B. Gradients in wood specific gravity of trees. Bull. Torr. Bot. Club 111, 51–55 (1996).
13. Hubbell, S. P. et al. Light-gap disturbances, recruitment limitation, and tree diversity in a neotropical forest. Science 283, 554–557 (1999).
14. West, G. B., Brown, J. H. & Enquist, B. J. A general model for the origin of allometric scaling laws in biology. Science 276, 122–126 (1997).
15. Enquist, B. J., Brown, J. H. & West, G. B. Allometric scaling of plant energetics and population density. Nature 395, 163–165 (1998).
16. West, G. B., Brown, J. H. & Enquist, B J. A general model for the structure and allometry of plant vascular systems. Nature 400, 664–667 (1999).
17. Peters, R. H. et al. The allometry of the weight of fruit on trees and shrubs in Barbados. Oecologia 74, 612–616 (1988).
18. Niklas, K. The allometry of plant reproductive biomass and stem diameter. Am. J. Bot. 80, 461–467 (1993).
19. Thomas, S. C. Reproductive allometry in Malaysian rain forest trees: biomechanics verses optimal allocation. Evol. Ecol. 10, 517–530 (1996).
20. Stevens, G. C. Lianas as structural parasites: the Bursera simaruba example. Ecol. 68, 77–81 (1987).
21. Whittaker, R. H. & Woodwell, G. M. Dimension and production relations of trees and shrubs in the Brookhaven Forest, New York. Ecology 56, 1–25 (1968).
22. Smith, D. W. & Tumey, P. R. Specific density and caloric value of the trunk wood of white birch, black cherry, and sugar maple and their relationship to forest succession. Can. J. For. Res. 12, 186–190 (1982).
23. Augspurger, C. K. Seed dispersal of the tropical tree Platyposdium elegans and the escape of its seedlings from fungal pathogens. J. Ecol. 71, 759–771 (1983).
24. Borchert, R. Soil and stem water storage determine phenology and distribution of Dry Tropical forest trees. Ecology 75, 1437–1449 (1994).
25. Sobrado, M. A. Aspects of tissue water relations of evergreen and seasonal changes in leaf water potential components of evergreen and deciduous species coexisting in tropical forests. Oecologia 68, 413–416 (1986).
26. Fearnside, P. M. Wood density for estimating forest biomass in Brazilian Amazonia. For. Ecol. Manage.

90, 59–87 (1997).
27. Janzen, D. H. Guanacaste National Park: Tropical Education, and Cultural Restoration (Editorial Univ. Estatal a Distanca, San Jose, 1986).
28. Niklas, K. J. Plant Allometry: The Scaling of Form and Process (Univ. Chicago Press, Chicago, 1994).
29. Harvey, P. H. & Pagel, M. D. The Comparative Method in Evolutionary Biology (Oxford Univ. Press, Oxford, 1991).
30. Malavassi, I. C. Maderas de Costa Rica: 150 Especies Forestales (Univ. de Costa Rica, San Jose, 1998).

....

Optimizing the success of random searches

G. M. Viswanathan*†‡, **Sergey V. Buldyrev***, **Shlomo Havlin***§, **M. G. E. da Luz**∥¶, **E. P. Raposo**∥# & **H. Eugene Stanley***

* Center for Polymer Studies and Department of Physics, Boston University, Boston, Massachusetts 02215, USA
† International Center for Complex Systems and Departamento de Física Teórica e Experimental, Universidade Federal do Rio Grande do Norte, 59072-970, Natal-RN, Brazil
‡ Departamento de Física, Universidade Federal de Alagoas, 57072-970, Maceió-AL, Brazil
§ Gonda-Goldschmied Center and Department of Physics, Bar Ilan University, Ramat Gan, Israel
∥ Lyman Laboratory of Physics, Harvard University, Cambridge, Massachusetts 02138, USA
¶ Departamento de Física, Universidade Federal do Paraná, 81531-970, Curitiba-PR, Brazil
# Laboratório de Física Teórica e Computacional, Departamento de Física, Universidade Federal de Pernambuco, 50670-901, Recife-PE, Brazil

....

We address the general question of what is the best statistical strategy to adapt in order to search efficiently for randomly located objects ('target sites'). It is often assumed in foraging theory that the flight lengths of a forager have a characteristic scale: from this assumption gaussian, Rayleigh and other classical distributions with well-defined variances have arisen. However, such theories cannot explain the long-tailed power-law distributions[1,2] of flight lengths or flight times[3-6] that are observed experimentally. Here we study how the search efficiency depends on the probability distribution of flight lengths taken by a forager that can detect target sites only in its limited vicinity. We show that, when the target sites are sparse and can be visited any number of times, an inverse square power-law distribution of flight lengths, corresponding to Lévy flight motion, is an optimal strategy. We test the theory by analysing experimental foraging data on selected insect, mammal and bird species, and find that they are consistent with the predicted inverse square power-law distributions.

Lévy flights are characterized by a distribution function

$$P(l_j) \sim l_j^{-\mu} \tag{1}$$

with $1 < \mu \le 3$, where l_j is the flight length. The gaussian is the stable distribution for the special case $\mu \ge 3$ owing to the central-limit theorem, while values $\mu \le 1$ do not correspond to probability distributions that can be normalized[2]. This generalization, equation (1), introduces a natural parameter μ such that we essentially have a

911

family of distributions. Our strategy is to find the value of the parameter—and hence the distribution—that optimizes the search process. Levandowsky *et al.*[3,4] have suggested why microorganisms may perform Lévy flights. A Lévy distribution is advantageous when target sites are sparsely and randomly distributed, irrespective of the value of μ chosen[7], because the probability of returning to a previously visited site is smaller than for a gaussian distribution. Another explanation, proposed by Shlesinger[6], argues that foragers may perform Lévy flights because the number of new visited sites is much larger for N Lévy walkers than for N brownian walkers[8–11]. A Lévy flight strategy is also a good solution for the related problem of where to locate N radar stations to optimize the search for M targets[12].

Here we develop an idealized model which captures some of the essential dynamics of foraging in the limiting case in which predator–prey relationships are ignored and learning is minimized. We assume that target sites are distributed randomly, and that the forager behaves as follows (see Fig. 1):

(1) If a target site lies within a 'direct vision' distance r_v, then the forager moves on a straight line to the nearest target site. A finite value of r_v, no matter how large, models the constraint that no forager can detect (or 'remember') a target site located an arbitrarily large distance away.

(2) If there is no target site within a distance r_v, then the forager chooses a direction at random and a distance l_j from the probability distribution (equation (1)). It then incrementally moves to the new point, constantly looking for a target within a radius r_v along its way. If it does not detect a target, it stops after traversing the distance l_j and chooses a new direction and a new distance l_{j+1}; otherwise, it proceeds to the target as in rule (1).

In the case of non-destructive foraging, the forager can visit the same target site many times. Non-destructive foraging can occur in either of two cases: if the target sites become temporarily depleted or fall below some fixed concentration threshold, and if the forager becomes satiated and leaves the area. In the case of destructive foraging, the target site found by the forager becomes undetectable in subsequent flights.

First, we solve this model analytically. Let λ be the mean free path of the forager between successive target sites (for two dimensions, $\lambda \equiv (2r_v\rho)^{-1}$ where ρ is the target-site area density). The mean flight distance is

$$\langle l \rangle \approx \frac{\int_{r_v}^{\lambda} l^{1-\mu} dl + \lambda \int_{\lambda}^{\infty} l^{-\mu} dl}{\int_{r_v}^{\infty} l^{-\mu} dl} \tag{2}$$

$$= \left(\frac{\mu-1}{2-\mu}\right)\left(\frac{\lambda^{2-\mu} - r_v^{2-\mu}}{r_v^{1-\mu}}\right) + \frac{\lambda^{2-\mu}}{r_v^{1-\mu}}$$
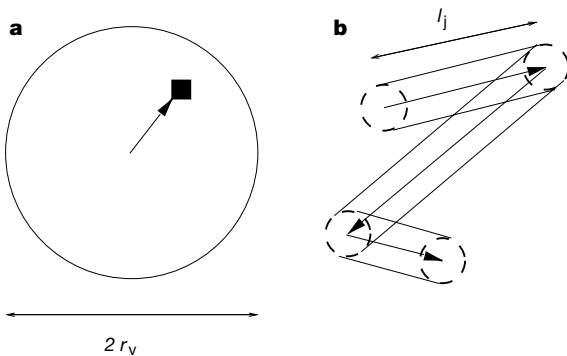

Figure 1 Foraging strategy. **a**, If a target site (solid square) is located within a 'direct-vision' distance r_v, then the forager moves on a straight line to it. **b**, If there is no target site within a distance r_v, then the forager chooses a random direction and a random distance l_j from the Lévy probability distribution $P(l_j) \sim l_j^{-\mu}$, and then proceeds as described in the text.

The second term of this 'mean field' calculation is approximate because it assumes that the distances λ_k between successive sites k are all equal to λ. The probability distribution has a finite cutoff λ and corresponds to a truncated Lévy distribution. An infinite λ leads to divergences for $\mu \leq 2$ (see Fig. 2a). The cutoff causes convergence to gaussian behaviour only after a very large number of steps[13]. A more rigorous treatment that considers a Poisson distribution of λ_k does not alter the results significantly (see simulation results below).

We define the search efficiency function $\eta(\mu)$ to be the ratio of the number of target sites visited to the total distance traversed by the forager, so that

$$\eta = \frac{1}{\langle l \rangle N} \tag{3}$$

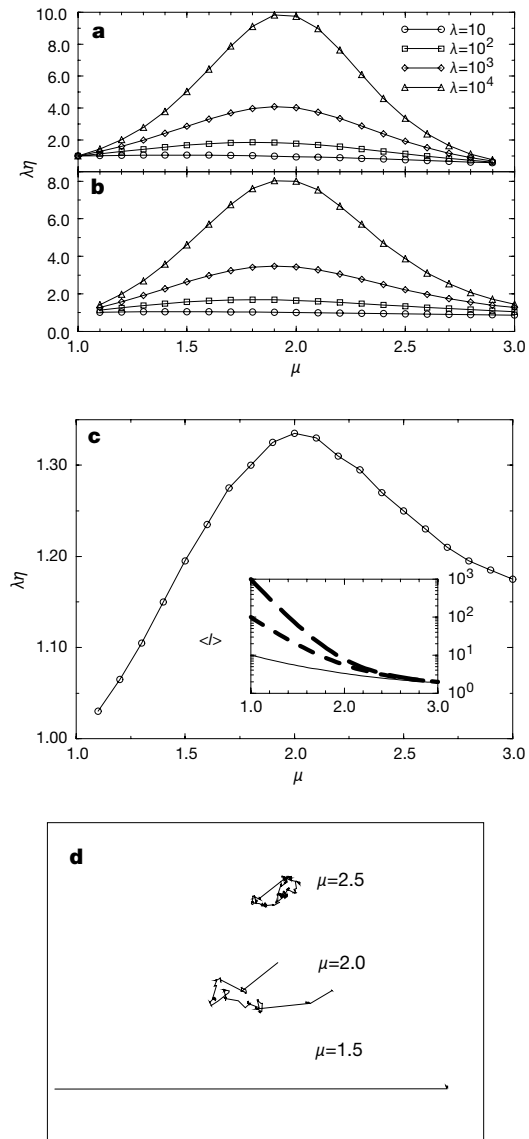where N is the mean number of flights taken by a Lévy forager while

Figure 2 a, **b**, The product of the mean free path λ and the foraging efficiency η against the Lévy parameter μ in one dimension for different values of λ, found from equations (2) and (3) ($r_v = 1$) for the case of non-destructive foraging (**a**) and from simulations (**b**). **c**, $\lambda\eta$ found from simulations in two dimensions, with $\lambda = 5,000$ ($r_v = 1$). In each case, $\mu_{opt} \approx 2$ emerges as an optimal value of the Lévy flight exponent. Inset shows $\langle l \rangle$ as a function of μ for $r_v = 1$ and $\lambda = 10$ (solid line), $\lambda = 10^2$ (dashed), $\lambda = 10^3$ (long-dashed). The results indicate that flights become too long when $\mu < 2$, causing inefficient foraging (see equation (3)). **d**, Two-dimensional random walks for $\mu = 2.5$, 2.0 and 1.5 with identical total lengths of 10^3 units.

travelling between two successive target sites. A low value of η can result from either a larger N or a large $\langle l \rangle$, corresponding to large and small μ, respectively. For intermediate values of μ it is thus conceivable that a maximum in η can arise. We first consider the case of destructive foraging. The mean number of flights N_d taken to travel an average distance λ between two successive target sites scales[14] as

$$N_d \approx (\lambda/r_v)^{\mu-1} \qquad (4)$$

for $1 < \mu \leq 3$. Here $\mu - 1$ is the fractal dimension of the set of sites
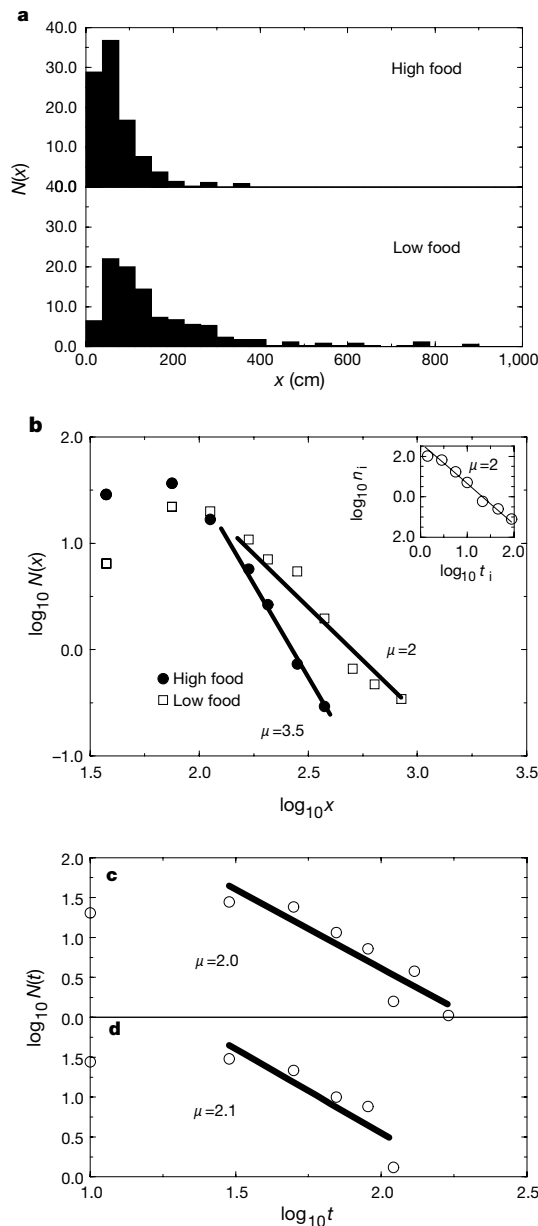
Figure 3 Foraging by bumble-bees and deer. **a**, Flight-length percentage distributions for foraging bumble-bees. We digitized the data from ref. 15. **b**, Double-log plot of the same data; the value $\mu \approx 2$ for low nectar concentration is the same as predicted by the model. We are interested solely in the long flights, because the power-law exponent μ is not affected by short flights. The value $\mu \approx 3.5$ for higher nectar concentrations (approximately 10 times) in which long flights become very rare (see text) is consistent with the prediction that η becomes independent of μ when $\lambda \leq r_v$. We smoothed the data using running averaging. The inset displays a double-log plot of the histograms of flight times (in 1-h intervals) for the wandering albatross[6]. **c**, **d**, Double-log plot of the foraging time (in s) percentage distributions for deer in wild areas (**c**) and fenced areas (**d**). We digitized the original data from ref. 16. In fenced areas, spatial limitation introduces an artificially larger number of 'turnings'.

visited by a Lévy random walker. (If the number of sites m in a closed region of a radius r scales as $m \approx r^{d_f}$, then d_f is the fractal dimension of the set of sites.) Note that $N_d \approx (\lambda/r_v)^2$ for $\mu \geq 3$ (brownian motion)[2]. We also consider the case of non-destructive foraging. Because previously visited sites can be revisited, equation (4) overestimates the mean number N_n of flights between successive target sites for the non-destructive case. We show below that $N_n \approx N_d^{1/2}$. Let r_o be the small distance between the last visited target site and the position after the first subsequent flight. For a brownian walker, in the case of destructive foraging, $N_d \approx \lambda^2$ because the average time required for a random walker in one dimension who is initially in the middle of a container of radius λ to reach the boundary is $N_d = \lambda^2/(2D)$, where D is the diffusion constant. However, for the non-destructive case, $N_n = (\lambda - r_o)r_o/(2D)$, because the previous site (only a small distance r_o away) can be revisited—that is, the scaling is quadratic in the former case and linear in the latter. We have found this result also to hold for anomalous diffusion and spatial dimensions higher than 1. It follows that

$$N_n \approx (\lambda/r_v)^{(\mu-1)/2} \qquad (5)$$

for $1 < \mu \leq 3$. We have also systematically tested equation (5) using simulations, and find that the approximation becomes increasingly better as (λ/r_v) increases (compare also Fig. 2a, b).

Having found expressions for N_d and N_n, we first consider the case in which the target sites are plentiful, that is, $\lambda \leq r_v$. Then $\langle l \rangle \approx \lambda$ and $N_d \approx N_n \approx 1$. Hence, η becomes independent of μ. This behaviour does not correspond to Lévy flight motion because long flights with $l_j \gg r_v$ are practically non-existent. We next study the more usual case in which the target sites are sparsely distributed, defined by $\lambda \gg r_v$. Substituting equations (2) and (4) into equation (3), we find for destructive foraging that the mean efficiency η has no maximum, with lower values of μ leading to more efficient foraging. Note that when $\mu = 1 + \epsilon$ with $\epsilon \to 0^+$, the fraction of flights with $l_j < \lambda$ becomes negligible, and effectively the forager moves along straight lines until it detects a target site. For non-destructive foraging, we note that if $\lambda \gg r_v$, then $N_d \gg N_n$. Substituting equations (2) and (5) into equation (3), and differentiating with respect to μ, we find that the efficiency $\eta = 1/(N_n\langle l \rangle)$ is optimum at

$$\mu_{opt} = 2 - \delta \qquad (6)$$

where $\delta \approx 1/[\ln(\lambda/r_v)]^2$. So, in the absence of *a priori* knowledge about the distribution of target sites, an optimal strategy for non-destructive foraging is to choose $\mu_{opt} = 2$ when λ/r_v is large but not exactly known.

We test the above theoretical results with numerical simulations, which have the advantage that no approximations are made. Specifically, we perform one- and two-dimensional simulations of the model and study how η varies with μ for the case of non-destructive foraging for a random distribution of target sites. Figure 2a shows that the simulation agrees with the analytical results (Fig. 2b), and approaches $\mu_{opt} = 2$ as $\lambda \to \infty$. The discrepancy in η near $\mu = 3$ is due to the slow convergence of N_n, which approaches the expected scaling behaviour as $\lambda \to \infty$. The simulation results for two dimensional non-destructive foraging also show maxima near $\mu_{opt} = 2$. Figure 2c shows simulated foraging in a system of size $10^4 \times 10^4$ with $r_v = 1$, periodic boundary conditions and $\lambda/r_v = 5 \times 10^3$. For destructive foraging with $\lambda \gg r_v$, simulations show that $\mu \to 1$ optimizes the efficiency as predicted. In contrast, if the target sites are densely distributed such that $\lambda \approx r_v$, then, as expected, we find no significant effect of varying μ. Our findings agree with the theoretical predictions and raise the possibility that Lévy-flight foraging with $\mu < 3$ may be confined to instances of low global target-site concentration, as the advantage of long flights becomes negligible when there are ample target sites (see also Figs 2b and 3b). Note that our simulation results do not suffer from the approximations inherent in equation (2).

We compare our analytical and simulation results with foraging

data on a variety of animals. The original foraging data on bees (Fig. 3a) were collected by recording the landing sites of individual bees[15]. We find that, when the nectar concentration is low, the flight-length distribution decays as in equation (1), with $\mu \approx 2$ (Fig. 3b). (The exponent μ is not affected by short flights.) We also find the value $\mu \approx 2$ for the foraging-time distribution of the wandering albatross[6] (Fig. 3b, inset) and deer (Fig. 3c, d) in both wild and fenced areas[16] (foraging times and lengths are assumed to be proportional). The value $2 \leq \mu \leq 2.5$ found for amoebas[4] is also consistent with the predicted Lévy-flight motion.

The above theoretical arguments and numerical simulations suggest that $\mu \approx 2$ is the optimal value for a search in any dimension. This is analogous to the behaviour of random walks whose mean-square displacement is proportional to the number of steps in any dimension[17]. Furthermore, equations (4) and (5) describe the correct scaling properties even in the presence of short-range correlations in the directions and lengths of the flights. Short-range correlations can alter the width of the distribution $P(l)$, but cannot change μ, so our findings remain unchanged. Hence, learning, predator–prey relationships and other short-term memory effects become unimportant in the long-time, long-distance limit. A finite λ ensures that the longest flights are not energetically impossible. Our findings may also be relevant to the study of population dynamics. Specifically, each value of μ is related to a different type of redistribution kernel[18]; for example, $\mu \geq 3$ corresponds to the normal (or similar) distribution, while $\mu = 2$ corresponds to a Cauchy distribution (see also ref. 19). Finally, note that non-destructive foraging is more realistic than destructive foraging because, in nature, 'targets' such as flowers, fish and berries are often found in patches that regenerate. Organisms are often in clusters for reproductive purposes, and sometimes such clusters may have fractal shapes[20]. Thus, the forager can revisit the same food patch many times. We simulated destructive foraging in various patchy and fractal target-site distributions and found results consistent with non-destructive foraging with uniformly distributed target sites. □

1. Tsallis, C. Lévy distributions. *Phys. World* **10**, 42–45 (1997).
2. Schlesinger, M. F., Zaslavsky, G. M. & Frisch, U. (eds) *Lévy Flights and Related Topics in Physics* (Springer, Berlin, 1995).
3. Levandowsky, M., Klafter, J. & White, B. S. Swimming behavior and chemosensory responses in the protistan microzooplankton as a function of the hydrodynamic regime. *Bull. Mar. Sci.* **43**, 758–763 (1988).
4. Schuster, F. L & Levandowsky, M. Chemosensory responses of *Acanthamoeba castellani*: Visual analysis of random movement and responses to chemical signals. *J. Eukaryotic Microbiol.* **43**, 150–158 (1996).
5. Cole, B. J. Fractal time in animal behaviour: The movement activity of *Drosophila. Anim. Behav.* **50**, 1317–1324 (1995).
6. Viswanathan, G. M. *et al.* Lévy flight search patterns of wandering albatrosses. *Nature* **381**, 413–415 (1996).
7. Shlesinger, M. F. & Klafter, J. in *On Growth and Form* (eds Stanley, H. E. & Ostrowsky, N.) 279–283 (Nijhoff, Dordrecht, 1986).
8. Berkolaiko, G., Havlin, S., Larralde, H. & Weiss, G. H. Expected number of distinct sites visited by N discrete Lévy flights on a one-dimensional lattice. *Phys. Rev. E* **53**, 5774–5778 (1996).
9. Berkolaiko, G. & Havlin, S. Territory covered by N Lévy flights on d-dimensional lattices. *Phys. Rev. E* **55**, 1395–1400 (1997).
10. Larralde, H., Trunfio, P., Havlin, S., Stanley, H. E. & Weiss, G. H. Territory covered by N diffusing particles. *Nature* **355**, 423–426 (1992).
11. Larralde, H., Trunfio, P., Havlin, S., Stanley, H. E. & Weiss, G. H. Number of distinct sites visited by N random walkers. *Phys. Rev. A* **4**, 7128–7138 (1992).
12. Szu, H. in *Dynamic Patterns in Complex Systems* (eds Kelso, J. A. S., Mandell, A. J. & Shlesinger, M. F.) 121–136 (World Scientific, Singapore, 1988).
13. Mantegna, R. N. & Stanley, H. E. Stochastic process with ultra-slow convergence to a gaussian: The truncated Lévy flight. *Phys. Rev. Lett.* **73**, 2946–2949 (1994).
14. Shlesinger, M. F. & Klafter, J. Comment on "Accelerated diffusion in Josephson junctions and related chaotic systems". *Phys. Rev. Lett.* **54**, 2551 (1985).
15. Heinrich, B. Resource heterogeneity and patterns of movement in foraging bumble-bees. *Oecologia* **40**, 235–245 (1979).
16. Focardi, S., Marcellini, P. & Montanaro, P. Do ungulates exhibit a food density threshold—a field-study of optimal foraging and movement patterns. *J. Anim. Ecol.* **65**, 606–620 (1996).
17. Berg, H. C. *Random Walks in Biology* (Princeton Univ. Press, Princeton, 1983).
18. Kot, M., Lewis, M. & van der Driessche, P. Dispersal data and the spread of invading organisms. *Ecology* **77**, 2027–2042 (1996).
19. Schulman, L. S. *Time's Arrows and Quantum Measurement* (Cambridge Univ. Press, Cambridge, 1997).
20. Sugihara, G. & May, R. Applications of fractals in ecology. *Trends Ecol. Evol.* **5**, 79–86 (1990).

Water stress inhibits plant photosynthesis by decreasing coupling factor and ATP

W. Tezara*, V. J. Mitchell†, S. D. Driscoll† & D. W. Lawlor†

* Instituto de Biologia Experimental, Facultad de Ciencias, Universidad Central de Venezuela, Calla Suapore, Colinas de Bello Monte, Apartado 47114, Caracas 1041a, Venezuela
† Biochemistry and Physiology Department, IACR-Rothamsted, Harpenden, Hertfordshire AL5 2JQ, UK

Water stress substantially alters plant metabolism, decreasing plant growth and photosynthesis[1-4] and profoundly affecting ecosystems and agriculture, and thus human societies[5]. There is controversy over the mechanisms by which stress decreases photosynthetic assimilation of CO_2. Two principal effects are invoked[2,4]: restricted diffusion of CO_2 into the leaf, caused by stomatal closure[6-8], and inhibition of CO_2 metabolism[9-11]. Here we show, in leaves of sunflower (*Helianthus annuus* L.), that stress decreases CO_2 assimilation more than it slows O_2 evolution, and that the effects are not reversed by high concentrations of CO_2[12,13]. Stress decreases the amounts of ATP[9,11] and ribulose bisphosphate found in the leaves, correlating with reduced CO_2 assimilation[11], but the amount and activity of ribulose bisphosphate carboxylase-oxygenase (Rubisco) do not correlate. We show that ATP-synthase (coupling factor) decreases with stress and conclude that photosynthetic assimilation of CO_2 by stressed leaves is not limited by CO_2 diffusion but by inhibition of ribulose biphosphate synthesis, related to lower ATP content resulting from loss of ATP synthase.

When land plants absorb less water from the environment through their roots than is transpired (evaporated) from their leaves, water stress develops. The relative water content (RWC), water potential (ψ) and turgor of cells are decreased and the concentrations of ions and other solutes in the cells are increased, thereby decreasing the osmotic potential[1-4]. Stomatal pores in the leaf surface progressively close[2,6,13,14], decreasing the conductance to water vapour (g_{H_2O}) and thus slowing transpiration and the rate at which water deficits develop[1-4,6,11,14]. Also, photosynthetic assimilation of CO_2 (A) decreases, often concomitant with, and frequently ascribed to, decreasing conductance to CO_2 (g_{CO_2}) (refs 2–4, 6, 8). However, decreased A is also considered to be caused by inhibition of the photosynthetic carbon reduction (Calvin) cycle[1,2,9,11], although there is uncertainty over which biochemical processes are most sensitive to stress[2,3,6,15,16]. We assessed whether A is controlled by g_{CO_2} or by metabolic factors by measuring CO_2 and O_2 exchange, using large CO_2 concentrations (up to 0.1 mol mol^{-1}, equivalent to 10% volume/volume) to overcome small g_{CO_2} (refs 8, 12–14), and by determining important indicators of photosynthetic biochemistry (for example, ribulose biphosphate (RuBP) and Rubisco of the Calvin cycle)[9,10,16,17]. We considered the role of ATP in particular[2,9,10] because, although inhibition of photophosphorylation has been demonstrated[9,10] but is not widely accepted[3,4,6,18,19], it may explain the decrease in RuBP and A (refs 2, 11).

In the chloroplasts of leaf cells, capture of photons causes electron transport in the thylakoid membranes, evolution of O_2 (refs 2–4)